STUDIA INFORMATICA 2004
Volume 25 Number 1 (57)

Katarzyna STĄPOR, Lesław PAWLACZYK
Politechnika Śląska, Instytut Informatyki
Magdalena TROJNAR
Wojewódzki Ośrodek Okulistyczny - Katowice

LOCATING EYE-CUP REGION IN FUNDUS EYE IMAGES FOR GLAUCOMA DIAGNOSING

Summary. In this paper a new algorithm of the eye cup segmentation from fundus eye images (fei) is proposed. It is based on an adaptive dynamic thresholding technique performed on a channel a* of a L*a*b* color model. The obtained contour of eye-cup region will be used in a classification procedure supporting ophthalmologist in glaucoma diagnosing.

Keywords: image segmentation, adaptive thresholding, glaucoma

AUTOMATYCZNA LOKALIZACJA WNĘKI NACZYNIOWEJ NA CYFROWYCH OBRAZACH DNA OKA DLA WSPOMAGANIA DETEKCJI JASKRY

Streszczenie. W artykule prezentowany jest nowy algorytm segmentacji cyfrowych obrazów dna oka (fei). Jest on oparty na adaptacyjnym progowaniu wykonywanym na kanale a* modelu kolorów L*a*b*. Uzyskany kontur wnęki naczyniowej jest używany w procedurze klasyfikacji wspomagającej lekarza okulistę w diagnostyce jaskry.

Słowa kluczowe: segmentacja obrazu, progowanie adaptacyjne, jaskra

1. Introduction

Glaucoma is a group of diseases characterized by the proceeding optic nerve neuropathy, which leads to the rising diminuition in vision field, ending with blindness. The correct eye disk contains *neuroretinal rim* of pink color placed on the *eye disk* circuit and centrally placed

yellowish *eye cup* (Fig. 3). Glaucomatus changes in retina appearance embrace various changes in neuroretinal rim and eye cup, as the result of nerve fibers damages.

Examination of the eye disk structures is one of the most important tasks in glaucoma diagnosis. Searching for glaucoma damages during routine examination (i.e. based on ophthalmoscope and slit lamp with Volk lens) is not an easy task and gives uncertain results even with the experienced ophthalmologist. Therefore, there is a need for objective methods of automatic eye disc structures localisation.

In the existing approaches to automatic segmentation of fundus eye images (**fei**) for supporting glaucoma examinations [1,3,7,9,10] researchers focused on the detection of the eye disk and its characteristics. In [5] important proofs that shape of the eye cup and its numerical characteristics correlate with progress of glaucoma disease were presented.

In this paper the new automatic segmentation method of the eye cup from fei is presented. The novelty lies in the automatic segmentation of the eye cup from fundus eye images, which wasn't the area of interest in the past. Fig. 1 shows the steps of the proposed eye cup segmentation algorithm. The next step will be a classification of digital fundus eye images (**fei**) into normal and glaucomatous ones, based on the suitable shape descriptors, which is a subject of our current work.

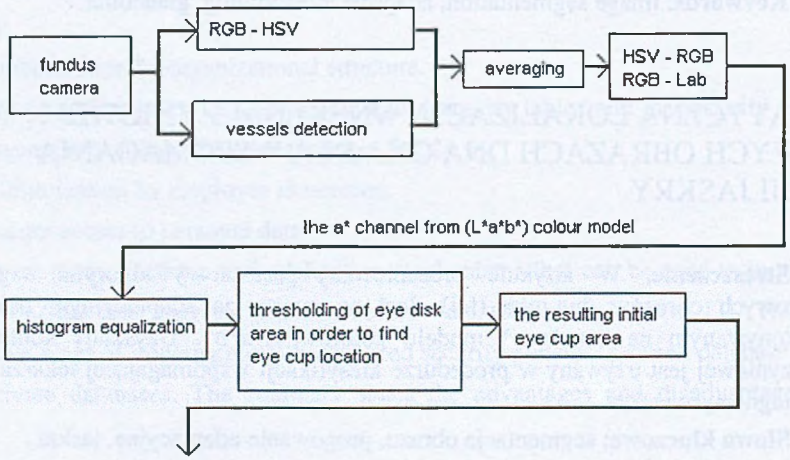

Fig. 1. Stages of the eye cup segmentation method
Rys. 1. Etapy segmentacji wnęki naczyniowej

2. Methods

Before the algorithm starts a user is asked to indicate a rectangle, which contains eye disk, to decrease the computation time.

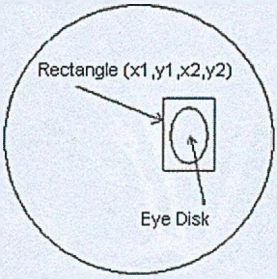

Fig. 2. Rectangle specified by user containing eye disk
Rys. 2. Prostokąt wskazany przez użytkownika zawierający wnękę naczyniową

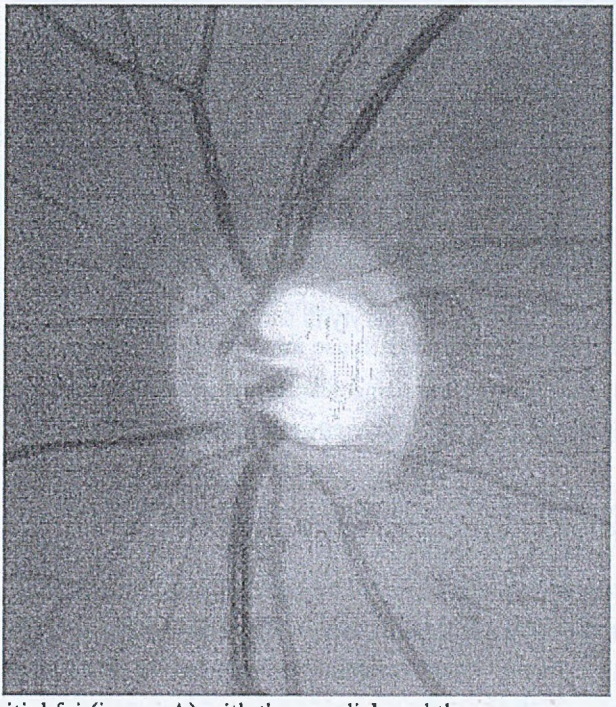

Fig. 3. The initial fei (image A) with the eye disk and the eye cup area in the central part
Rys. 3. Wstępna postać obrazu (obraz A) z widocznym dyskiem optycznym oraz wnęką naczyniową w centralnej części

2.1. Vessels averaging

The algorithm for vessels averaging is based on the method of vessels detection described in [1]. An example of image with the detected vessels is shown in Fig. 4.

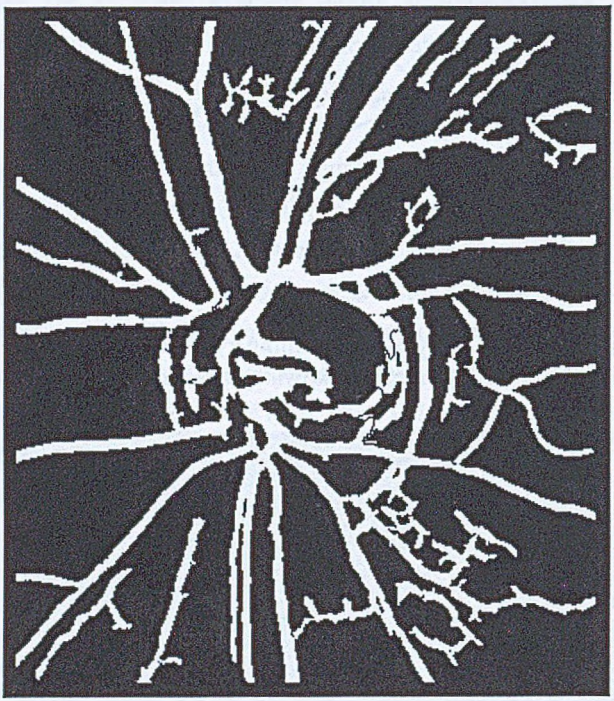

Fig. 4. Image A with the detected vessels
Rys. 4. Obraz A z wykrytymi naczyniami krwionośnymi

All white pixels (i.e. pixels comprising vessels) lying inside the user rectangle belong to the subregion named here $R_{eyecup-vessels}$. First, the input image is converted form RGB to HSV color model [2,4]. By overlying the image with detected vessels on the input, converted image, all border pixels of the detected vessels are found (subregion $R_{eyecup-vessels}$). For each border pixel in $R_{eyecup-vessels}$ its new color components $[H_{avg}, S_{avg}, V_{avg}]$, being the average of the appropriate components of pixels lying in the 8-connected neighborhood outside of $R_{eyecup-vessels}$ region are found. After recalculation of all border pixels, they are deleted, new border pixels are found and the process is repeated until size of $R_{eyecup-vessels}$ is higher than 0.

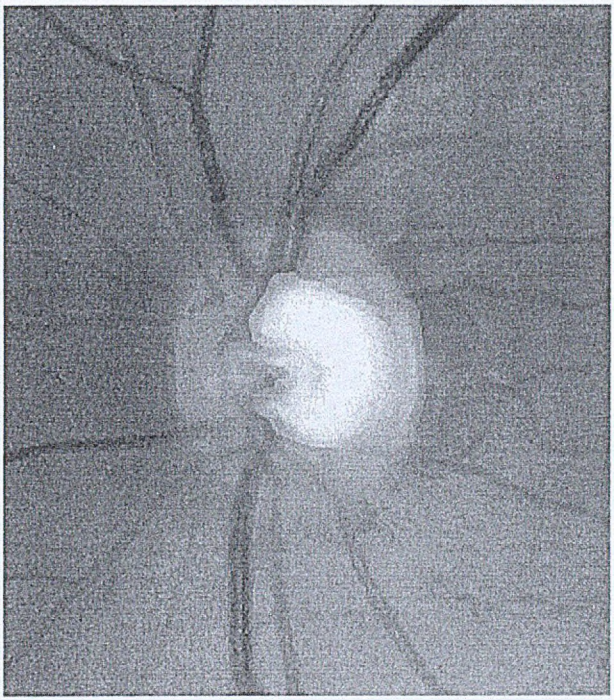

Fig. 5. Averaging vessels in the eye disk area from image A
Rys. 5. Uśrednianie naczyń krwionośnych w obrębie dysku optycznego na obrazie A

2.2. Image color model conversions

Color is perceived by humans as a combination of three primary colors: R (red), G (green) and B (blue). From R, G, B representation we can derive other kinds of color models (spaces) by using either linear or non-linear transformations.

Two color spaces are used in the presented segmentation algorithm: *HSV* and (L*, a* ,b*) [2].

HSV color space is composed of three channels: *H* (Hue) represents basic colors, *S* (Saturation) is a measure of a purity of a color and *V* (Value) is a measure of intensity. Color information is represented by hue and saturation values, while intensity, which describes the brightness of image is represented by value component. There are algorithms for transformation RGB into HSV coordinates [4].

The main goal was to find a proper color model, which could distinguish the eye cup from the rest of fei. During examinations of different color models, *L*a*b** color space was found the best for this purpose. It can be derived through CIE XYZ color space [2] from RGB model.

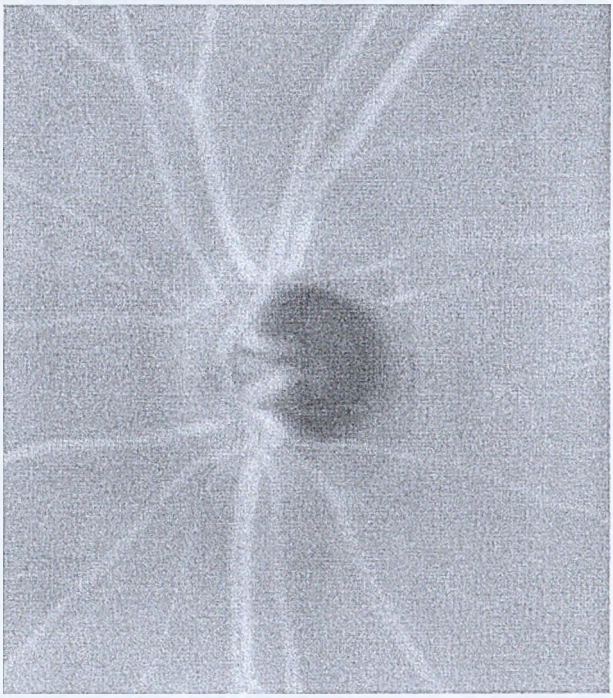

Fig. 6a. Channel a* of sampled fei A
Rys. 6a. Kanał a* przykładowego obrazu A

CIE (Commision International de l'Eclaraige) [2,4] color model has three primaries denoted as X, Y, Z. Any color can be specified by the combination of X, Y, Z. The values of X, Y, Z can be computed by a linear transformation from RGB tristimulus coordinates.

$$\begin{bmatrix} X \\ Y \\ Z \end{bmatrix} = \begin{bmatrix} 0.607 & 0.174 & 0.200 \\ 0.299 & 0.587 & 0.114 \\ 0.000 & 0.066 & 1.116 \end{bmatrix} \begin{bmatrix} R \\ G \\ B \end{bmatrix}$$

The $(L^*,a,^*b^*)$ model can be computed through CIE XYZ color model as follows:

$$L^* = 116\left(\sqrt[3]{\frac{Y}{Y_o}}\right) - 16$$

$$a^* = 500\left[\sqrt[3]{\frac{X}{X_o}} - \sqrt[3]{\frac{Y}{Y_o}}\right]$$

$$b^* = 200\left[\sqrt[3]{\frac{Y}{Y_o}} - \sqrt[3]{\frac{Z}{Z_o}}\right]$$

$YY_0 > 0.01$, $X/X_0 > 0.01$, $Z/Z_o > 0.01$ and (X_0, Y_0, Z_0) are (X,Y,Z) values for standard white. The values of X,Y,Z can be computed by a linear transformation from RGB tristimulus coordinates.

In Figs. 6 a, b channels a^* and b^* of a sampled fei A are shown. It's evident, that the best for further examinations is the channel a^*. It's observable, that the eye cup appears as a dark part and is the only element in the image with such a low luminance.

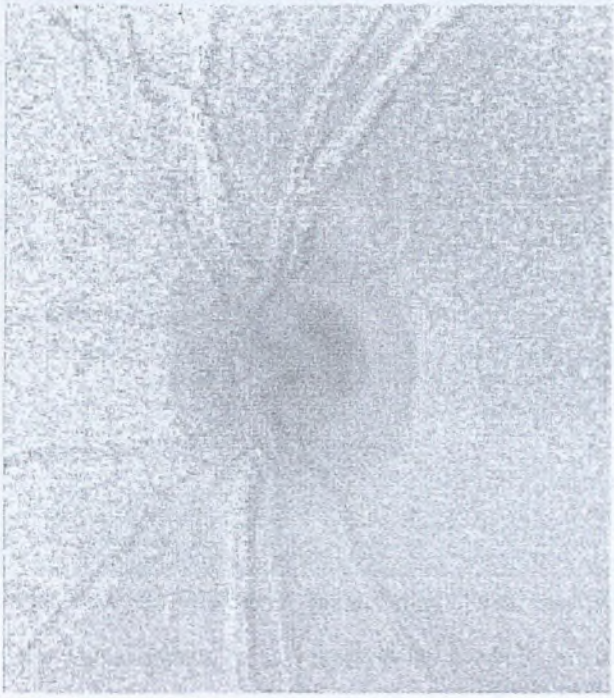

Fig. 6b. Channel b* of sampled fei A
Rys. 6b. Kanał b* przykładowego obrazu A

2.3. Histogram equalization

Let r_1, ..., r_L (L defines number of all levels) denote the intensity values (color) in the image. The histogram creates a set of values: $p(r_1)$, ..., $p(r_L)$ evaluated by the formula:

$$p(r_j) = n_j/n$$

where n_j is the number of pixels in image characterized by intensity level r_j and n is the number of all pixels in image.

The histogram equalization transformation [4] is given by the function:

$$s_k = T(r_k) = \sum_{j=1}^{k} p(r_j), \; k=1,2, ..., L$$

The result of using this transformation is a histogram much more equalized, which uses the whole set of intensity levels.

The operation of histogram equalization is executed on the a^* component of a $L^*a^*b^*$ model (Fig 6a) to improve the image contrast.

2.4. Image thresholding

Thresholding provides a way to separate out the regions of the image corresponding to objects in which we are interested, from the regions of the image that correspond to background. It is an operation, that involves tests against a function T of the form [4]:

$$T = T[x,y,p(x,y),f(x,y)],$$

where f(x,y) is the gray level of point (x,y) and p(x,y) denotes some local property of this point – for example the average gray level of a neighborhood centered at (x,y). A thresholded image g(x,y) is created by defining:

$$g(x,y) = \begin{cases} 0 & f(x,y) \le T \\ 1 & f(x,y) > T \end{cases}$$

where T is a threshold. Pixels labeled 1. When T depends only on f(x,y), the threshold is called global. In adaptive thresholding, for each pixel in an image, a threshold has to be calculated. Adaptive methods are particularly useful in the cases where there is a large range of variation in gray scale from one part of the image to another, so that a single fixed threshold cannot be used for the entire image. There are two main approaches to finding a local threshold [4]:

1) Dynamic thresholding

Finding a local threshold by statistically examining the intensity values of a local neighborhood of each pixel. The statistic, which is the most appropriate, depends largely on the input image.

2) Local thresholding

Divides an image into an array of subimages and then finds the optimum threshold for each subimage by investigating its histogram. The threshold for each single pixel is found by interpolating the results of the subimages. The drawback of this method is that it is computationaly expensive.

The resulting image (i.e. channel a^*) with the equalized histogram is a subject of the proposed adaptive dynamic thresholding method. A local threshold is found by statistically examining the intensity values of a local neighborhood of each pixel. A window centered at each pixel is constructed as its local neighborhood. The statistic used is a function:

$$T = M_{mean} - C$$

where M_{mean} is a mean of gray level values, C is a constans, experimentally set. The size of the neighborhood has to be large enough to cover sufficient foreground and background pixels,

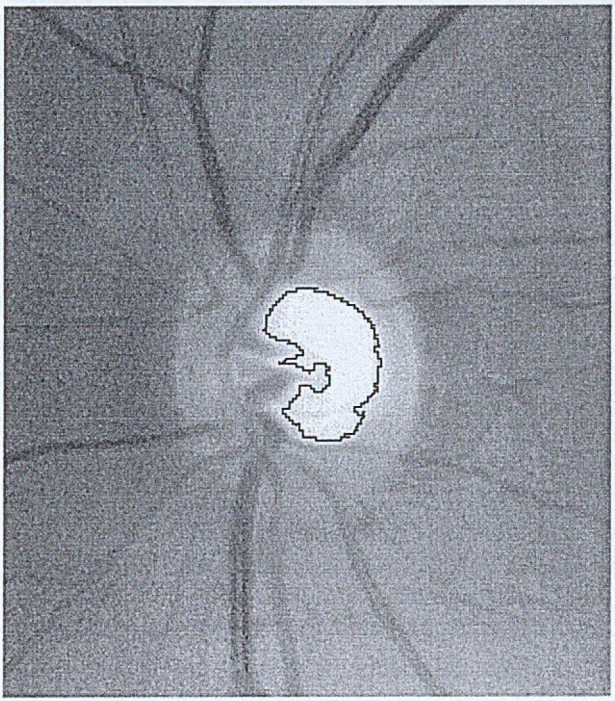

Fig. 7. Thresholding results of image A using the calculated table of thresholds shown in Fig. 8

Rys. 7. Wyniki progowania obrazu A przy korzystaniu z tabeli progów pokazanej na rys. 8

otherwise a poor results are obtained. On the other hand, choosing regions which are too large can violate the assumption of a uniformity. In our case window of size 120x120 with the value of C equal to 20 is used.

Fig 8 shows the resultant table of thresholds, while Fig 7 presents the result of the adaptive thresholding using the table of thresholds from Fig 8.

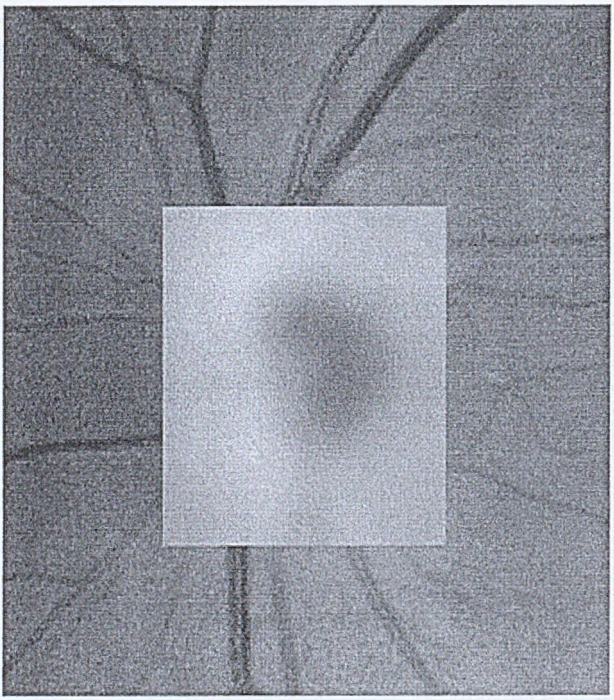

Fig. 8. Table of thresholds generated by the algorithm
Rys. 8. Tablica progów stworzonych przez algorytm

3. Experimental results and conclusions

The new method has been applied into 50 fei of patients with glaucoma, which where previously examined by conventional methods (perimetry, slit lamp with Volk lens) and 50 fei of normal patients. On the acquired from Canon CF-60Uvi fundus camera images, the eye cup contour is automatically detected. During the thresholding a window of size 120 x 120 and the value of C equal to 20 are used.

Fig 3 shows the sampled fundus eye image, while Figures 4 through 8 show the results of the successive stages of the presented method.

Fig 4 presents the detected blood vessels, Fig 5 the result after vessels averaging and Figures 6a and 6b channels a* and b* of the image shown in Fig 3. Fig 8 shows the table of thresholds generated by the thresholding algorithm. Figure 7 presents the boundary of the eye cup region (solid line) obtained as a result of thresholding the image (i.e. a channel a*) shown in Figure 6 using a table of thresholds shown in Fig 8.

It is important to note that contours of the eye-cup obtained as a result of the presented segmentation method coincide with the contour marked by an ophthalmologist. The results of using the presented method are very encouraging.

The feature extraction of the suitable eye-cup shape descriptors as well as a classification of the segmented fundus eye images into normal and glaucomatous ones are now being developed.

REFERENCES

1. Chaudhuri S., Chatterjee Sh., Katz N., Nelson M., Goldbaum M.: Detection of Blood Vessels in Retinal Images Using Two-Dimensional Matched Filter. IEEE Transactions on Medical Imaging, Vol 8, No. 3, September 1989.
2. Cheng H. D. at all: Color image segmentation: advances and prospects. Pattern Recognition, Vol. 34, No 3, p. 2259-2281, 2001.
3. Goh K. G., et al: ADRIS: an Automatic Diabetic Retinal Image Screening system. K. J. Cios (Ed.): Medical Data Mining and Knowledge Discovery, pp 181-210, Springer-Verlag New York, November 2000.
4. Gonzalez R. C., Woods R. E.: Digital Image Processing, Prentice-Hall, 2002.
5. Jonas J. B., Budde W. M., Panda-Jonas S.: Ophthalmoscopic evalutation of the optic nerve head. Survey of Ophthalmology, Vol. 43, Nb. 4 January – February 1999.
6. Kanski J. et al.: Glaucoma. A color manual of diagnosis and treatment. Butterworth-Heinemann, 1996.
7. Morris D. T., Donnison C.: Identifing the Neuroretinal Rim Boundary Using Dynamic Contours. Image and Vision Computing 17 (1999), pp. 169-174.
8. Nakagawa Y., Rosenfeld A.: „Some experiments on variable thresholding", Pattern Recognition, vol. 11, pp. 191-204, 1979.
9. Osareh A., Mirhmedi M., Thomas B., Markham R.: Classification and Localisation of Diabetic Related Eye Disease. A. Heyden et al. (Eds.): ECCV 2002, LNCS 2353, pp. 502-516, 2002.
10. Sinthanayothin Ch.: "Image Analysis for Automatic Diagnosis of Diabetic Retinopathy". Phd Thesis, University of London, 1999.

Recenzent: Dr inż. Bogdan Smołka

Wpłynęło do Redakcji 9 czerwca 2003 r.

Abstract

W artykule przedstawiono nowy algorytm automatycznej segmentacji wnęki naczyniowej na cyfrowych obrazach dna oka. Składa się on z następujących faz: konwersje modeli kolorów (rys. 1), uśrednianie naczyń krwionośnych (rys. 5), opcjonalne poprawienie kontrastu i dynamiczne progowanie adaptacyjne (rys. 8). W progowaniu adaptacyjnym korzysta się z odpowiedniej statystyki, którą jest średnia wartość poziomu szarości w oknie wyśrodkowanym na każdym punkcie, modyfikowana przez stałą.

Znalezione zaproponowanym algorytmem segmentacji kontury wnęki naczyniowej pokrywają się z tymi, które wskazał lekarz okulista. Ekstrakcja cech wnęki jak i deskryptory kształtu oraz klasyfikacja segmentowanych obrazów na kategorie chorych i zdrowych są obecnie przedmiotem dalszych badań.

Adresses

Katarzyna STĄPOR: Politechnika Śląska, Instytut Informatyki, ul. Akademicka 16, 44-101 Gliwice, Polska, delta@ivp.iinf.polsl.gliwice.pl .

Lesław PAWLACZYK: Politechnika Śląska, Instytut Informatyki, ul. Akademicka 16, 44-101 Gliwice, Polska, palles@polsl.gliwice.pl .

Magdalena TROJNAR, Wojewódzki Ośrodek Okulistyczny, ul. Powstańców 31, 40-129 Katowice.